Combined interpolation—restoration of Landsat images through FIR filter design techniques

L. M. G. FONSECA, G. S. S. D. PRASAD
and N. D. A. MASCARENHAS

Instituto Nacional de Pesquisas Espaciais, Avenue dos Astronautas 1758, 12201 São José dos Campos, S. P., Brasil

(Received 12 July 1989; in final form 9 October 1992)

Abstract. In digital image processing for remote sensing there is often a need to interpolate an image. Examples occur in scale magnification, image registration, geometric correction, etc. On the other hand, this image can be subject to several sources of degradation and it would be interesting to compensate also for this degradation in the interpolation process. Therefore, this article addresses the problem of combining interpolation and restoration in a single operation, thereby reducing the computational effort. This is done by means of two-dimensional, separable, Finite Impulse Response (FIR) filters. The ideal low pass FIR filter for interpolation is modified to account for the restoration process. The Modified Inverse Filter (MIF) and the Wiener Filter (WF) are used for this purpose. The proposed methods are applied to the interpolation-restoration of Landsat-5 Thematic Mapper data. The later process takes into account the degradation due to optics, detector and electronic filtering. A comparison with the Parametric Cubic Convolution (PCC) technique is made. The experimental results consist of interpolation-restoration processes of Landsat-5 Thematic Mapper images from 30 m to 15 m (scale magnification) but they could also be generalized to include deblurring on more general interpolation problems, like geometric correction

1. Introduction

The resolution of images obtained by satellite sensors is degraded by sources, such as: optical diffraction, detector size and electronic filtering. As a consequence, the effective resolution is, in general, worse than the nominal resolution, that corresponds to the detector projection on the ground and does not take into consideration the sensor imperfections.

Through resoration techniques, it is possible to improve image resolution up to a certain level. This paper explores the idea of combining the restoration process with an interpolation process to generate images with a better resolution over a finer grid than the original sampling grid. Related works in this area include those of Seto *et al.* (1990), Malaret (1985), Kalman (1984), Wilson (1979), Dye (1975).

The combined interpolation-restoration process is performed by means of two-dimensional, separable, Finite Impulse Response (FIR) filters. The ideal low pass FIR filter for interpolation (Crochiere and Rabiner 1983) is modified to account for the restoration process. The proposed method is applied to the interpolation-restoration of Landsat-5 Thematic Mapper (TM) data.

2. The problem of image restoration

The image restoration problem attempts to recover an image that has been degraded by the limited resolution of the sensor as well as by the presence of noise.

0143–1161/93 $10.00

In sensors like the Multi-spectral Scanner (MSS) or the Thematic Mapper (TM), the image is obtained in digital form so there is a need to incorporate the sampling process in the model. A useful model that has been proposed for the recording process in such systems is given by

$$g_\Lambda = [f * h + n] \cdot S_\Lambda, \tag{1}$$

where f represents the original scene, h is the point spread function (PSF) of the sensor, n is the additive noise, S_Λ is the sampling function and g_Λ is the sampled image.

In the Fourier domain this equation can be rewritten as

$$G_\Lambda(u) = \frac{1}{\Delta x} \sum_n F(u - nu_a) H(u - nu_a) + N_\Lambda(u) \tag{2}$$

where G_Λ, F, H and N_Λ are the Fourier transforms of g_Λ, f, h and n_Λ, respectively and Δx is the sampling period.

The objective of image restoration is to design a filter $P(u)$, periodic with period u_a, such that, when convolved with expression (1), the effect of $H(u - n_a)$ is cancelled, i.e.,

$$H(u)P(u) = 1 \quad |u| \leqslant u_c \tag{3}$$
$$0 \quad \text{elsewhere}$$

where u_c is the cut-off frequency of H.

An obvious choice for $P(u)$ is the inverse filter:

$$P(u) = \frac{1}{H(u)} \quad |u| \leqslant u_c \tag{4}$$

However, the inverse filter is unstable (Pratt 1978), (Rosenfeld and Kak 1982). The instability arises from the location of the zeroes of $H(u)$.

The Modified Inverse Filter (MIF), also called Transfer Function Compensation (TFC), approximates the inverse filter and at the same time attempts to control the problems associated with it. The proposed MIF is based on the work of (George and Smith 1962), (Sellner 1971) and (Arguello, Sellner and Stuller 1972).

The idea is to choose a desired function D as the response of the system, that would alleviate the ill-conditioning effects.

$$D = H \cdot P \tag{5}$$

The function D should have a better behaviour than the function H. A constant value for D yields the inverse filter. Once D is selected, P can be estimated:

$$P(u) = \frac{D(u)}{H(u)} \quad |u| \leqslant u_c \tag{6}$$
$$0 \quad \text{otherwise}$$

The selection of the desired function is discussed in §4.

It may be noted that the Wiener filter has a similar form to (6) (Andrews and Hunt 1977)

$$P(u) = \frac{1}{H(u)} \left[\frac{|H(u)|^2}{|H(u)|^2 + \dfrac{S_n(u)}{S_f(u)}} \right] \tag{7}$$

One of the major difficulties in using the Wiener filter is that the power spectral densities of signal (S_f) and noise (S_n) are not always known *a priori*. Therefore, the ratio S_n/S_f is approximated empirically by a constant K_w (Gonzalez and Wintz 1987). This type of filter given in (8) was also used in the study.

$$Pw(u) = \frac{1}{H(u)} \left[\frac{|H(u)|^2}{|H(u)|^2 + K_w} \right] \tag{8}$$

3. Analysis of the combined interpolation-restoration process

In digital image processing, the technique that is used to estimate sample values of an image over a desired grid, from samples over the original grid, is known as resampling. Conventional techniques such as the Nearest-Neighbor, Bilinear and Parametric Cubic Convolution (PCC) have been used by the remote sensing community in order to perform this interpolation process (Bernstein 1975, Park and Schowengerdt 1983). On the other hand, the interpolation process can also be regarded from the digital signal processing point of view (Crochiere and Rabiner 1983), (Câmara Neto and Mascarenhas 1983). Using this approach, interpolation can be efficiently performed by FIR filters.

This FIR filter approximates the ideal interpolation filter, with transfer function given by

$$H_I(u) = \begin{cases} 1 & |u| \leqslant u_c \\ 0 & \text{outside,} \end{cases} \tag{9}$$

where u_c is the maximum frequency of the analogue signal.

If the original signal was subject to degradation by blur and corruption by additive noise, it is possible to combine the processes of interpolation and restoration in a single filtering operation.

Consider two different sampling grids Λ_1 and Λ_2. The model for the combined process, illustrated in figure 1 below, by using the interpolation and restoration filters, can be written as

$$\hat{f}_{\Lambda_2} = g_{\Lambda_1} * [q_{\Lambda_2} * p_{\Lambda_2}], \tag{10}$$

where q and p are the interpolation and restoration filters, respectively. The subscripts Λ_1 and Λ_2 are used to define the input and output sampling grids, respectively.

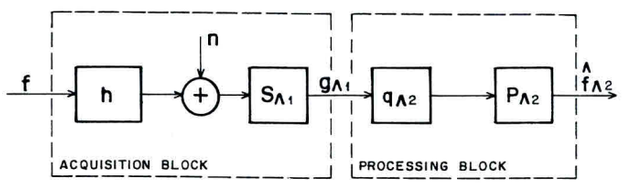

Figure 1. Model for the combined process of restoration—interpolation.

The image formation model presented in figure 1 is the so-called continuous-discrete model (Andrews and Hunt 1977). This model is considered to be more realistic to represent the data acquisition process. On the other hand, only approximations of the continuous object are possible with digital processing. Therefore, the discrete-discrete model will be used in the following. In the absence of noise, the sampled and degraded signal, g, is related to the original signal over the same grid, f_{Λ_1}, by:

$$g_{\Lambda_1}=h_{\Lambda_1}*f_{\Lambda_1} \tag{11}$$

By substituting (11) in (10) and by calculating the Discrete Fourier Transform, one obtains:

$$F_{\Lambda_2''}=F_{\Lambda_1''}H_{\Lambda_1''}Q_{\Lambda_2''}P_{\Lambda_2''}=F_{\Lambda_1''}H'_{\Lambda_2''}, \tag{12}$$

where Λ'' is the reciprocal of the sampling grid and

$$H'_{\Lambda_2''}=[H_{\Lambda_1''}Q_{\Lambda_2''}]P_{\Lambda_2''}. \tag{13}$$

From (13) it is observed that the restoration filter $P_{\Lambda_2''}$ must compensate the effects of $H_{\Lambda_1''}$ and $Q_{\Lambda_2''}$ to obtain a good approximation of $F_{\Lambda_2''}$. By combining the interpolation ($Q_{\Lambda_2''}$) and restoration ($P_{\Lambda_2''}$) processes into a single convolution operation, it is possible (Dye 1975) to reduce the computational cost of the solution.

4. Design of the interpolation-restoration filter by FIR windowing techniques

4.1. *Specification of the MIF filter*

The design of the MIF filter requires knowledge of the transfer function of the sensors. The transfer function (or the point spread function) of the MSS and the TM have been experimentally determined by several authors for the entire imaging system (Anuta *et al.* 1984), Malaret *et al.* 1985), as well as the contribution of each component (optics, detector and filters) (Markham, 1985). In the present study, the transfer function for both MSS and TM was approximated as a separable Gaussian function, i.e.,

$$H(u)=\exp(-Ku^2) \tag{14}$$

where u is the normalized frequency with respect the sampling frequency u_s, and K a function of the Equivalent Instantaneous Field of View (EIFOV):

$$K=4\ln(2)u_s^2(\text{EIFOV})^2 \tag{15}$$

The values of EIFOV used for MSS and TM are given in tables 1 and 2 respectively, which were obtained by using the models proposed by Markham (1985) and Park *et al.* (1984). The desired response $D(u)$ was chosen as

Table 1. EIFOV (in m) for MSS.

Bands direction	1-4
x	86·21
y	121·47

Table 2. EIFOV (in m) for TM.

Bands direction	1-4	5·7	6
x	41·6	40·5	168·9
y	45·4	45·4	179·0

$$D(u)=1 \qquad 0\leqslant u\leqslant u_w \tag{16}$$
$$0{\cdot}5(1+\cos[\pi(u-u_w)/(u_c-u_w)]) \quad u_w\leqslant u\leqslant u_c$$

where u_c is the system cut-off, and u_w the frequency for which the MTF of the imaging system is 0·5.

Figure 2 below displays the desired response and the approximated gaussian model for the MTF of the TM sensor (Bands 1-4).

The design of the separable digital filter was accomplished through the windowing technique. Different window shapes (Shlien, Cosine, Hann and Kaiser) were tested. For all the window shapes the transition bandwidth was increased due to the convolution operation in the frequency domain, corresponding to the multiplication of the window in the spatial domain (Oppenheim and Schafer 1975). There are very little differences in the desired frequency response $D(u)$ obtained through different window shapes (for $N=13$), as shown in figure 3. Moreover, the subjective differences between interpolated-restored images with different window shapes were insignificant.

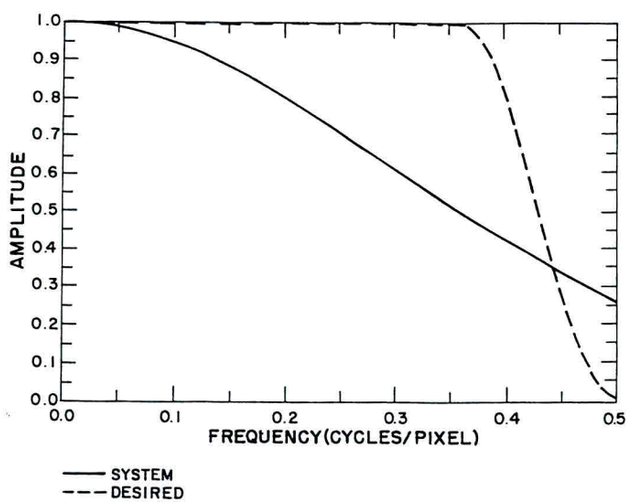

Figure 2. Desired response and the approximated Gaussian model for the MTF of the TM sensor. ——, system; ----, desired.

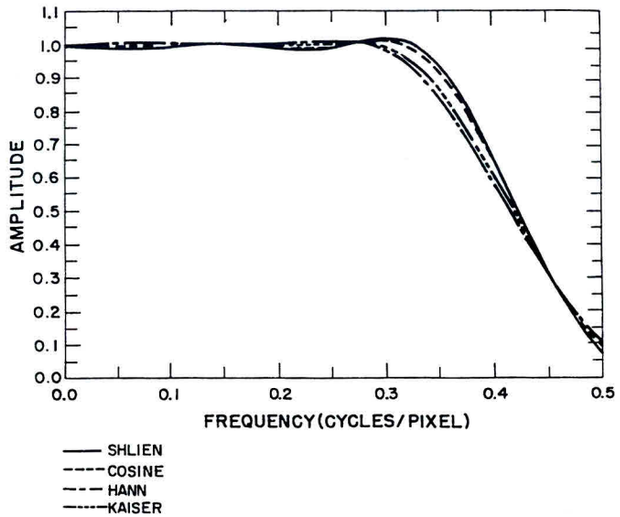

Figure 3. Effect of truncation ($N=13$) on the desired function for different windows. ——, Shlien; – – – –, Cosine; — — —, Hann; — — — — —, Kaiser.

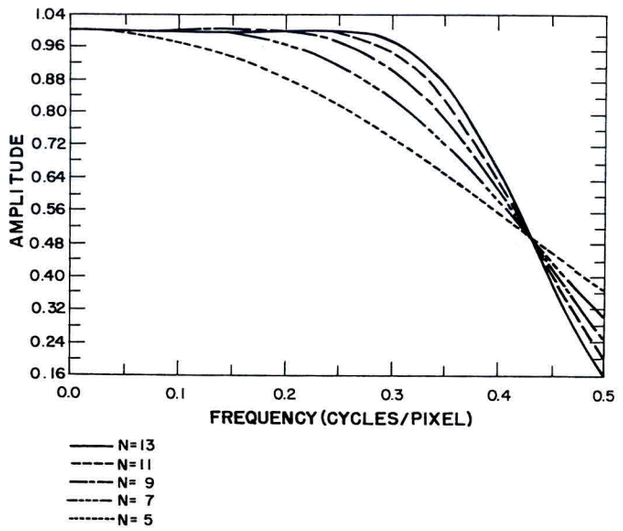

Figure 4. Effect of truncation (Hann window) for different values of N. ——, $N=13$; — — —, $N=11$; — — —, $N=9$ — — — — —, $N=7$; – – – –, $N=5$.

One way to evaluate the effect of truncating the impulse response of the filter through a window is to compare the desired function for several truncating sizes. Figure 4 displays curves of the desired function obtained for truncating sizes equal to 13, 11, 9, 7 and 5, with the Hann window.

It can be seen that the truncation of the filter impulse response by windowing causes an attenuation of the desired function that increases as the filter size decreases. This is more evident for $N<9$. This was verified through experiments, which showed that images that were processed with filters with size down to 9 by 9 did not display significant differences. For a 256 by 256 region of the TM image with small details, histograms of the difference between processed images with filter sizes 13, 11 and 9 (Hann window) were computed. More than 92 per cent of the pixels had grey levels between -2 and $+2$. Therefore, an interpolation-restoration filter with $N=9$ is sufficient to generate images with good visual quality, since the use of longer filters increases the computational cost without a significant improvement.

4.2. *Design of the Wiener filter*

The Wiener filter was implemented in its approximate form, where the noise-to-signal ratio S_n/S_f is substituted by a constant (8). Figure 5 displays the responses of the Wiener filter ($K_w=0{\cdot}1$) and MIF ($u_w=0{\cdot}36$) without truncation. It can be observed that the Wiener filter attenuates the response in the region where the signal-to-noise ratio is high, that is, in the neighbourhood of $u=0$. The use of a smaller K_w in order to alleviate this problem implies the increase of the response near the Nyquist frequency and a noisy image is obtained.

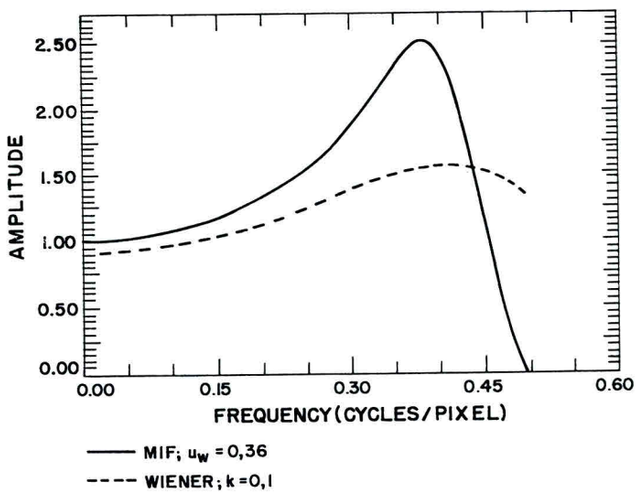

Figure 5. Restoration filters: Wiener and MIF. ——, MIF; $u_w=0{\cdot}36$; – – – –, Wiener; $K=0{\cdot}1$.

4.3. *Some implementation issues*

Crochiere and Rabiner (1983) present the basic concepts of periodically shift variant digital systems to modify the sampling rate of a sequence. In this section, we examine some aspects of the implementation of a FIR shift variant filter structure that are used in the design of a restoration filter, for interpolation-decimation by a factor M/L.

Once the frequency response of the restoration filter P is specified, the filter coefficients are obtained by the Inverse Fourier Transform of P, given by

$$p_n = \frac{1}{u_s}\int_0^{u_s} P(u)e^{j2\pi u_n}du, \tag{17}$$

where u_s is the sampling frequency.

The coefficients of the FIR restoration filter are obtained over a sampling rate which is L times greater than the sampling rate of the input sequence. If the size of the filter is N (odd), the number of filter coefficients, N_c, is given by

$$N_c = (N-1)L+1 \tag{18}$$

In actual implementation, only half of this number of coefficients are generated, due to the filter symmetry.

The integral given by Expression (17) is numerically calculated, through Simpson's rule (Rice 1983).

The filter coefficients are normalized. One must assure that

$$\sum_n p(n) = 1, \tag{19}$$

in order that the image average value should not be changed. As there are L sets of coefficients for the digital filter, for each set the normalization is made such that the validity of expression (19) is assured. It should be observed that this type of implementation of the restoration-interpolation of the FIR filter is equivalent to a polyphase network (Crochiere and Rabiner 1983).

The programme for the computation of the coefficients of the digital restoration-interpolation filter of Landsat images was developed in C language on a IBM-PC compatible microcomputer.

5. Experimental results

The 512 by 512 TM image that was used as a test in the study covers the Galeão International Airport, in Rio de Janeiro, Brazil, and was taken on 8 August 1987. The original image has only skew geometrical correction.

The images (Bands 1–4, 5 and 7) were resampled over a 15 m spaced grid through the restoration-interpolation method and the interpolation by PCC (Parametric Cubic Convolution) with $=-0{\cdot}5$ (Park and Schowengerdt, 1983). In order to evaluate the restored images, these images were compared to the images that were interpolated by PCC.

5.1. *Visual quality*

Figures 6–8 correspond to the sequence of TM images (Band 3) that display a comparison between the interpolated and restored images (512 by 512 pixels). The differences between figures 7 and 8 are mainly on the edges or objects that exhibit more contrast with respect to surrounding areas. Linear features appear more enhanced in the restored image.

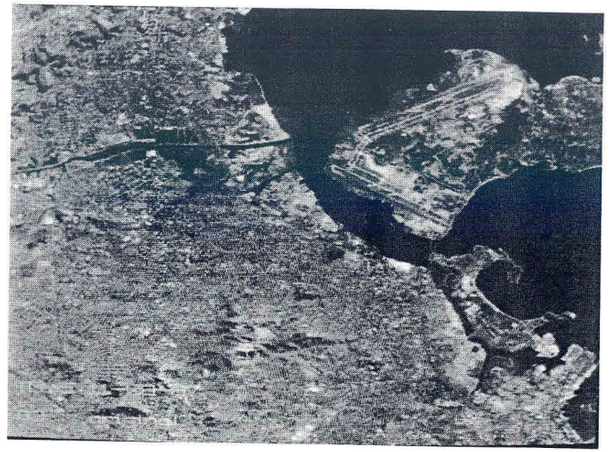

Figure 6. TM original image (512 by 512)—Band-3, pixel = 30 m. A region of 256 by 256 pixels was taken for resampling.

The parametric cubic convolution process attenuates the high frequency components of the image and, therefore, a more blurred image is obtained. On the other hand, the restoration process amplifies the high frequency components of the image and an image with sharper transitions is obtained.

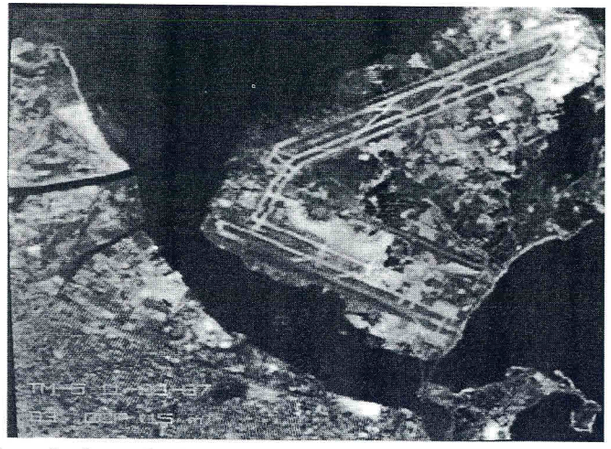

Figure 7. Interpolated image-parametric cubic convolution pixel = 15 m.

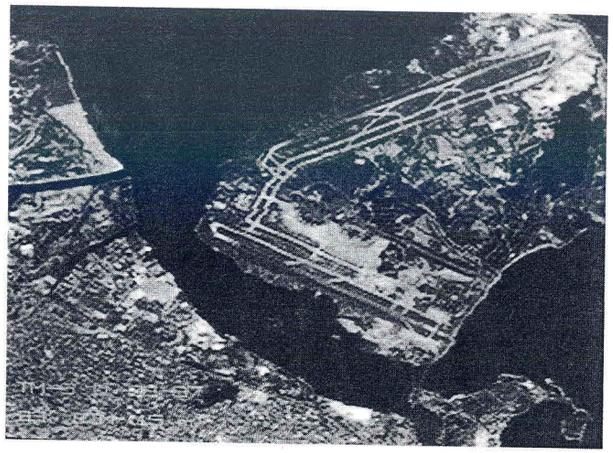

Figure 8. Restored-interpolated image—pixel = 15 m.

One can also observe that street delineation is better in the restored image, although the enhancement of the Moiré effect (aliasing) is also more evident in the restored image. This effect is clear on the edges of the airport runways that, instead of being linear, appear in a sawtooth form. In the interpolated image this effect also appears, but in a less pronounced form. The greater Moiré effect in the restored image is due to the fact that the restoring filter amplifies the high frequencies, that were folded over low frequency bands (spectrum overlap) in the sampling process.

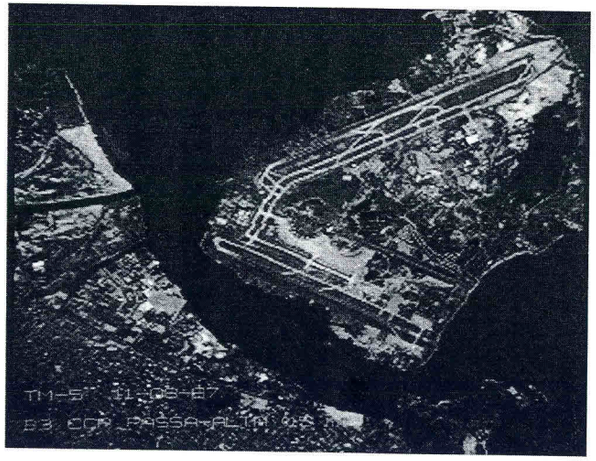

Figure 9. High-Pass filtering of PCC.

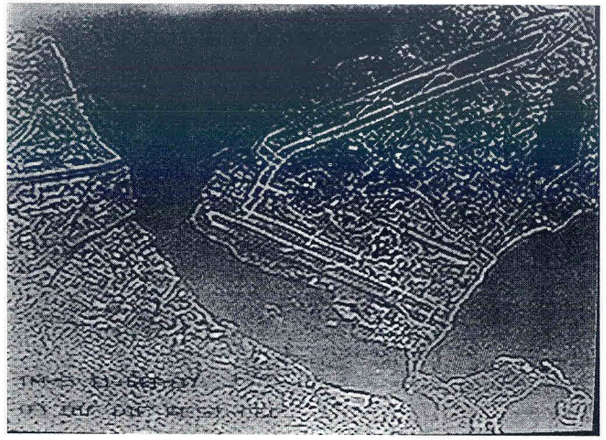

Figure 10. Difference image (Band 3) with contrast stretch.

One experiment was also performed by applying a 3 by 3 high-pass, separable conventional filter after the parametric cubic convolution interpolation.

This 3 by 3 filter has the following form:

$$\begin{bmatrix} -1 \\ 3 \\ -1 \end{bmatrix} [-1 \quad 3 \quad -1] = \begin{bmatrix} 1 & -3 & 1 \\ -3 & 9 & -3 \\ 1 & -3 & 1 \end{bmatrix} \tag{20}$$

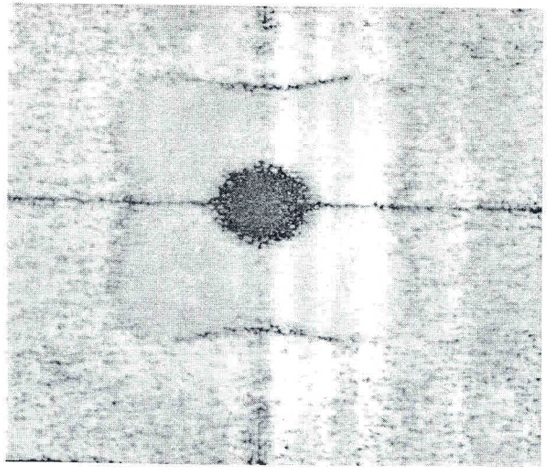

Figure 11. Ratio-image (restored/cubic convolution) of the Fourier Transform.

The corresponding one-dimensional Discrete Fourier Transform is given by:

$$H(u) = 3 - 2\cos 2\pi u \qquad 0 \leqslant u \leqslant 1/2 \tag{21}$$

Figure 9 displays the result. It can be observed that a greater detail rendition is obtained, as compared to figure 8, at the expense of more aliasing and noise amplification (particularly over water), as well as additional computational effort.

5.2. *Difference between images*

The difference image was obtained through a pixel-by-pixel subtraction (figure 7 minus figure 8) and taking the absolute value of this difference. The largest differences occur on the edges between high contrast areas (airport runways, for example), as it can be observed through figure 10.

The cubic convolution process presents a blurring effect: the low pixel values corresponding to the dark side of an object are slightly increased and the high tones, corresponding to the bright side of the border, are reduced. The restoration process decreases the smoothing effect, produces sharper transitions on the edges and increases the overall sharpness of the image. These results are in accordance with the visual analysis of the original images.

5.3. *Fourier analysis*

A Fast Fourier Transform routine was used to compute the two-dimensional transform of a 256 by 256 pixel sub-image of the resampled image (Band 3) by both methods. The ratio between the logarithms of the absolute values of the transformed restored and interpolated images was computed.

Figure 11 displays the ratio-image (Band 3) of the selected image.

Grey	$r < 0{\cdot}95$	(high frequencies)
Dark	$0{\cdot}95 \leqslant r \leqslant 1{\cdot}05$	(low frequencies)
White	$r > 1{\cdot}05$	(middle frequencies)

One can observe that the frequency content of the images using both resampling methods are approximately equal in the low frequencies region (dark region), as it was expected. In the middle frequencies, the ratio is greater than 1·05 for a large band of the spectrum (white region), since the frequency response of the restoration filter is greater than the PCC filter in the range $|u| \leqslant 0{\cdot}5$; in this region the frequency contents of the restored image is greater than that of the interpolated image. The grey band that appears close to the image boundary is a consequence of the fact that the PCC filter has a significant response beyond the cut-off system frequency, $u_c = 0{\cdot}5$. These components are responsible for the spectrum amplification of the interpolated image, in a region where it should have been eliminated by the interpolation filter in the ideal situation.

5.4. *Restoration-interpolation through the Wiener filter*

Figure 12 displays the restored-interpolated image (grid spacing = 15 m) by using the Wiener filter technique, according to (8). The choice of the parameter K_w was dictated by a compromise: small values of K_w imply an approximation to the inverse filter, with increase in the noise content of the restored image; large values of K_w imply an attenuation of the low frequency components of the image. A value of K_w equal to 0·1 was chosen after some experimentation and, as can be observed from

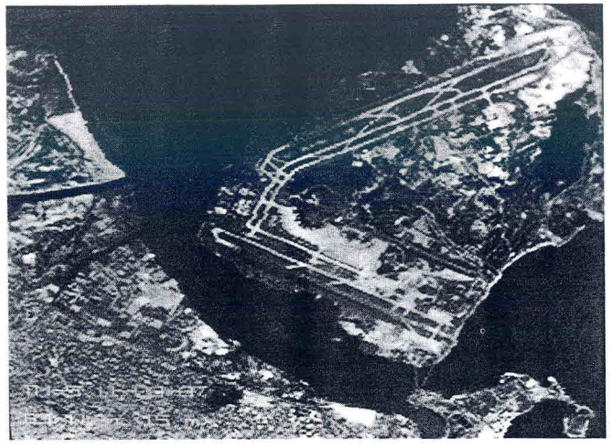

Figure 12. Restored-interpolated image by the Wiener Filter—pixel = 15 m.

figure 12, the corresponding visual results are similar to those of the Modified Inverse Filter.

5.5. *Restoration without interpolation*

Figure 13 shows the result of the restoration of figure 6 by using the Modified Inverse Filter without any interpolation. By comparing both figures, it is possible to notice some improvements in detail rendition, as in street delineation, for example.

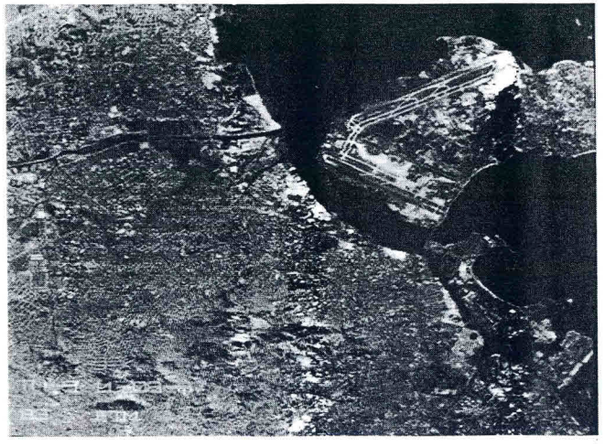

Figure 13. Restored image by MIF without interpolation—pixel = 30 m.

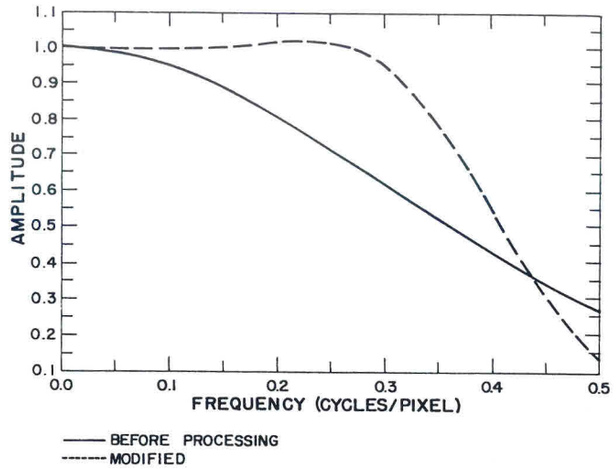

Figure 14. Response of the TM (Bands 1-4) modified by the MIF-Hann Window, $N = 11$. ——, Before processing; – – – –, Modified.

One can observe that the visual improvements are more evident when the restoration is combined with the interpolation process.

6. Concluding remarks

This work presented a restoration technique that is combined with the resampling process in order to interpolate Landsat satellite images. This was accomplished through the design of a Finite Impulse Response (FIR) filter that has input and output signals with different sampling rates.

An improvement of the spatial resolution of the sensor was obtained through the restoration process. By using the curves of the modified transfer function obtained from (13), (see figure 14) one obtains the EIFOV of the processed system. These values were determined as approximately 36·5 m and 38·0 m for Bands 1-4 and 36·3 m and 38·0 m for Bands 5 and 7, on the x and y directions, respectively. These results are better than those presented in table 2, as a result of the restoration process.

Acknowledgment

The authors wish to acknowledge the help of Dr Gerald J. F. Banon for valuable discussions about the subject of image restoration.

References

ANDREWS,. H. C., and HUNT, B. R., 1977, *Digital Image Restoration* (Englewood Cliffs, N.J.: Prentice Hall).

ANUTA, P. E., BARTOLUCCI, L. A., DEAN, M. E., LOZANO, D. F., MALARET, E., MCGILLEM, C. D., VALDES, J. A., and VALENZUELA, C. R., 1984, Landsat-4 MSS and Thematic Mapper data quality and information content analysis. *I.E.E.E. Transactions on Geoscience and Remote Sensing*, **22,** 222-238.

ARGUELLO, R. J., SELLNER, H. R., and STULLER, J. A., 1972, Transfer function compensation of sampled imagery, *I.E.E.E. Transactions on Computer*, **21,** 812-818.

BERNSTEIN, R., 1974, All-digital precision processing of ERTS images; final report. Greenbelt, MD, NASA, GSFC (NAS5-21716).

CÂMARA NETO, G., and MASCARENHAS, N. D. A., 1983, Methods for image interpolation through FIR filter design techniques. *Proceedings of the I.E.E.E. International Conference on ASSP*, (New York: I.E.E.E.), pp. 391-394.

CROCHIERE, R. E., and RABINER, L. R., 1983, *Multirate Digital Signal Processing* (Englewood Cliffs, N.J.: Prentice Hall).

DYE, R. H., 1975, Restoration of Landsat images by two dimensional convolution, *Proceedings of the 10th International Symposium on Remote Sensing of Environment* (Ann Arbor: ERIM), pp. 725-730.

GEORGE, C. F., and SMITH, H. W., 1962, The application of inverse convolution techniques to improve signal response of recorded geophysical data. *Proceedings of the IRE*, **50,** 2313-2319.

GONZALEZ, R. C., and WINTZ, P., 1987, *Digital Image Processing* (Reading, MA: Addison Wesley), 2nd edition.

KALMAN, L. S., 1984, Comparison of cubic-convolution interpolation and least-squares restoration for resampling Landsat MSS imagery, Unpublished Report, Technicolor Government Services, Inc.,

MALARET, E. R., 1985, Methods of image restoration for incoherent and coherent systems, Ph.D. Thesis, Purdue University, School of Electrical Engineering.

MALARET, E. R., BARTOLUCCI, L. A., LOZANO. D. F., ANUTA, P. E., and MCGILLEM, C. D., 1985, Landsat-5 Thematic Mapper data quality analysis. *Photogrammetric Engineering and Remote Sensing*, **51,** 1407-1416.

MARKHAM, B. L., 1985, The Landsat sensor's spatial responses. *I.E.E.E. Transactions on Geoscience and Remote Sensing*, **23,** 864-875.

OPPENHEIM, A. V., and SCHAFER, R., 1975, *Digital Signal Processing* (Englewood Cliffs: Prentice Hall).

PARK, S. K., SCHOWENGERDT, R., and KACZYNSKI, M., 1984, Modulation transfer function analysis for sampled image systems. *Applied Optics*, **23,** 2572-2582.

PARK, S. K., and SCHOWENGERDT, R. A., 1983, Image reconstruction by parametric cubic convolution. *Computer Vision, Graphics and Image Processing*, **23,** 258-272.

PRATT, W. K., 1978, *Digital Image Processing* (New York: Wiley).

RICE, J. R., 1983, *Numerical Methods, Software, and Analysis* (Tokyo, Japan: McGraw-Hill).

ROSENFELD, A., and KAK, A. C., 1982, *Digital Picture Processing* (New York: Academic).

SELLNER, H. R., 1971, Transfer function compensation of sampled imagery. In *A Symposium on Sampled Images* (Norwalk, Connecticut: Perkin Elmer).

SETO, Y., KOMURA, F., and HAMANO, N., 1990, A proposal of an interpolation filter with image quality correction capability. *Systems and Computers in Japan*, **21,** 43-57.

WILSON, C. L., 1979, Image mapping software at ERIM, *Proceedings of the Annual International User's Conference on Computer Mapping Hardware, Software and Data Bases, Cambridge, MA.*